A Passive Aerodynamic Strategy for Sustainable Mobility: Harnessing Biomimetic Dimpling to Improve Vehicle Fuel Economy

Jonathan Yi-Chen Cheng [1,*], Alec Chang [1], and Hsiu-Ju Chang [2]

[1]Taipei European School, Taipei, Taiwan
[2]Taipei Municipal Chien Kuo Senior High School, Taipei, Taiwan

[*]Correspondence: jonathan.chengb2028@stu.tes.tp.edu.tw

December 20, 2025

Abstract

This study explores biomimetic surface dimpling as a passive aerodynamic strategy for sustainable vehicle design. Inspired by natural flow control mechanisms, a 1:30 scale car model was developed with varying dimple depths (1.25, 2.5, and 5 mm) and placements (top, side, bottom). Ten high-precision SLA 3D-printed prototypes were tested in a custom-built subsonic wind tunnel at 2.7 m/s, with lift and drag forces measured using calibrated load cells and validated through computational fluid dynamics (CFD) simulations. We observed that side-mounted dimples with a 2.5 mm depth achieved optimal performance, reducing aerodynamic drag by approximately 25% compared to the smooth control model. CFD visualizations confirmed coherent streamwise vortices that delayed flow separation and enhanced pressure recovery, demonstrating the effectiveness of this mechanism. As a zero-energy passive modification, this approach directly supports UN Sustainable Development Goals 7 and 9 by improving energy efficiency and reducing emissions. The findings establish a scalable, nature-inspired framework for advancing vehicle aerodynamics, offering immediate applications for both electric and conventional vehicles in achieving sustainable mobility.

Keywords: Aerodynamic, Biomimetic dimpling, Sustainable mobility

1 Introduction

During a golf training session, it was discovered that the dimples on the golf ball greatly affect its flight trajectory. The dimples on the ball's surface appear

to play a critical role in extending its flight distance and controlling its spin and curvature. To verify this observation, the dimpled outer layer was removed to reveal a smooth-surfaced ball for testing; the results were striking. Both the backspin rate and flight distance dropped dramatically, demonstrating that the dimples significantly influence aerodynamic behavior.

This unexpected outcome raises a broader question in fluid dynamics and engineering design: could similar surface structures be applied to vehicles to reduce aerodynamic drag and improve energy efficiency? As global transportation accounts for a major share of energy consumption and carbon emissions, even a small reduction in drag can meaningfully contribute to sustainable mobility.

Therefore, this study investigates how the depth and configuration of surface dimples affect the drag coefficient of a small-scale vehicle model (Figure. 1). It is hypothesized that a moderate dimple depth will induce micro-turbulence that delays flow separation, thereby lowering the drag coefficient without requiring any additional energy input. This research aims to integrate biomimetic surface engineering principles into passive aerodynamic strategies that support energy-efficient and sustainable transport design.

2 Literature Review & Theoretical Framework

2.1 Aerodynamics of normal cars

As a car moves forward, air strikes the front bumper, slows down, and forms a high-pressure stagnation point before splitting to travel over and around the body. Along the car's smooth surfaces, a thin boundary layer develops (Kaushik et al., 2018). Initially, this boundary layer is laminar, but as the air flows over rougher surfaces, such as the windshield or roof, it can transition to turbulent flow. As the airflow continues and encounters sharp angles or an adverse pressure gradient, particularly near the rear window or trunk, it may no longer remain attached, leading to flow separation. This detachment creates a turbulent wake of low pressure behind the vehicle, producing most of the aerodynamic drag that resists forward motion (Tarakka et al., 2023; Mat et al., 2025). To reduce drag and improve fuel efficiency, various control methods are being explored, including the use of dimples.

2.2 Biomimetic dimpling

The inspiration for using dimples comes from the passive flow control of golf balls. A golf ball typically travels at speeds high enough to reduce its drag to approximately half that of a smooth sphere. This favorable reduction in drag is due to the dimples on the golf ball's surface, which trigger the boundary layer to transition from laminar to turbulent flow (Alam et al., 2011). This transition to turbulent flow within the boundary layer allows the air to remain attached to the surface for a longer distance around the golf ball, delaying flow separation and thereby reducing the size of the low-pressure wake behind it. As a result,

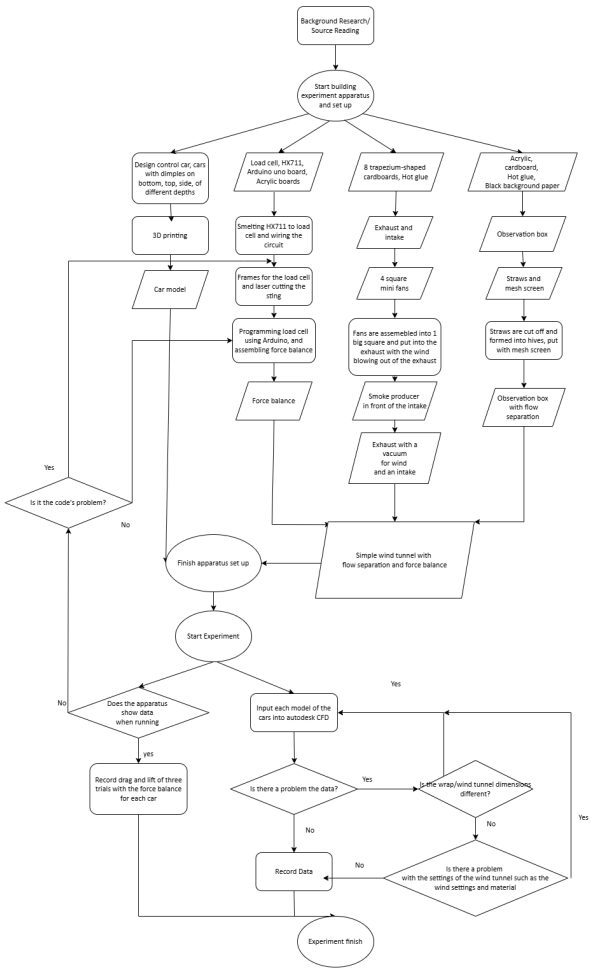

Figure 1: Experiment workload.

the pressure drag acting on the ball is significantly decreased, improving its aerodynamic efficiency and allowing it to travel farther.

Dimples are a passive flow control method involving techniques centered around adding supplementary structures to the body or making slight modifications to the body's geometric shape (Ali et al., 2024). Using the same logic as a golf ball, they create turbulence that enhances near-wall momentum exchange, delays flow separation, reduces wake size, and thereby reduces pressure drag. These effects are typically quantified by a decrease in drag coefficient (C_d) and an increase in lift-to-drag ratio (L/D). Incorporating dimples on a streamlined object like an airfoil may help delay flow separation and minimize wake size, thereby reducing pressure drag, but it could potentially result in increased friction drag, presenting a trade-off.

This investigation is motivated by a fundamental biomimetic principle observed in nature: the use of controlled surface roughness for drag reduction, as exemplified by the golf ball. The aerodynamics of a golf ball are well understood; its dimples reduce drag by promoting boundary layer transition, which delays flow separation and shrinks the low-pressure wake (Alam et al., 2011). This principle is not merely an isolated sports curiosity but is recognized as a canonical case of biomimetics, demonstrating how morphological design can optimize fluid dynamic performance (Obayashi et al., 2007). While preliminary studies have explored the feasibility of applying dimples to commercial vehicle surfaces (Palanivendhan et al., 2021), a comprehensive understanding of the synergistic effects of dimple location and depth remains limited. Therefore, this study aims to refine and apply this bio-inspired principle through a systematic parametric investigation, seeking an optimal configuration for vehicle drag reduction.

2.3 Dimples on aircraft and engineering

It has been shown that dimples can effectively reduce drag by up to 6.6% at all angles of attack when employed on aircraft wings. Additionally, research has indicated that an outward dimple structure is ineffective for reducing the drag coefficient under any circumstances. Therefore, a decision was made to avoid using an outward dimple structure and to implement an inward dimple structure instead (Ali et al., 2024). Furthermore, it has been demonstrated that the lift coefficient can be enhanced by dimples at most angles of attack, even reaching 3.87 at certain angles (Kaushik et al., 2018). However, despite the benefits dimples can provide, most aircraft today do not incorporate them. This may be due to the fact that under varying conditions, such as air pressure, flow velocity, and dynamic viscosity, the Reynolds number for the aircraft changes, which in turn alters the effects of the dimples. Consequently, if dimples are to be fully employed on aircraft, their design would need to be adjusted for each flight to correspond to the specific Reynolds number (Yu et al., 2023).

2.4 Dimples on ground vehicles and sustainable goals

Research has also been conducted on the effects of dimples on ground vehicles such as bullet trains and cars. For example, studies have examined the impact of dimples on the drag coefficients of cars. By exploring various factors related to the dimples, such as depth and location, it has been shown that the drag coefficient of cars decreases to a certain degree overall, regardless of how the features of the dimples are altered (Shaw et al., 2020). Furthermore, research has demonstrated that dimples on cars can also reduce lift coefficients, which is a desired outcome for vehicle performance (Ballerstein & Horst, 2023). However, their findings contradicted those of Kaushik et al. and Shaw et al., so whether dimples actually produce lift will need to be investigated further in additional experiments. Overall, despite the benefits that dimples can provide for cars, their effects are too minimal for practical implementation. This may be due to costs or the potential discomfort they could cause.

Even if the improvements are small, applying simple technology directly supports sustainable transportation goals. Reducing drag by just a few percent translates to significant fuel savings and lower CO_2 emissions across millions of vehicles, supporting SDG 7 (Affordable and Clean Energy) and SDG 13 (Climate Action). Improved aerodynamic efficiency also contributes to SDG 9 (Industry, Innovation, and Infrastructure) by promoting cleaner engineering innovations that optimize energy use without requiring additional materials or power. Moreover, research on textured surfaces can be integrated into electric vehicle design, extending battery range and reducing the frequency of charging, further enhancing energy efficiency and sustainable urban mobility.

3 Methods

3.1 Building a model car

As the test subject, a generic commercial car was built using Autodesk Fusion software (Figure. 2), resulting in a roughly 1:30 scaled-down model, which is commonly used for wind tunnel testing of ground vehicles (Li et al., 2021; Kacem & Abdullah, 2016). By adjusting the proportions of the vehicle, each area can accommodate 67 or 68 dimples to control the affected area of localized turbulence. After creating the shell of the car, the model is imported into Blender software to add depth and volume to the shell. In total, 10 models were produced (Figure. 3): a control model without dimples and 9 others, each with different dimple depths (1.25 mm, 2.5 mm, 5 mm) and locations (top, side, bottom), as different locations and depths of dimples can have varying effects on airflow (Ali et al., 2025).

The dimples were created using the Autodesk Fusion model by forming a large mesh grid of 0.5 cm cells across the desired surfaces and dragging a vertex bounded by four cells downward to the desired depth. This results in a hybrid dimple with V-shaped and semi-circular elements and rounded edges (Figure. 4); however, as the radius of the dimples remains constant, the slope of the sides

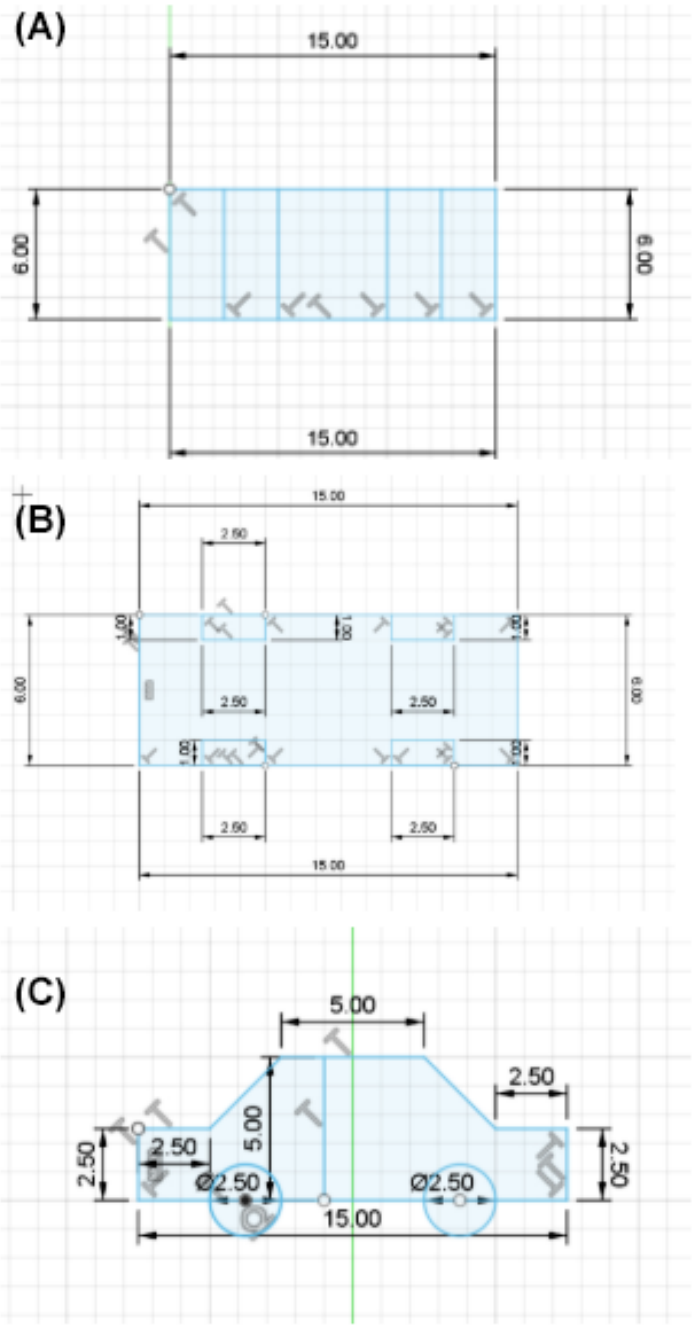

Figure 2: (A) Top profile of the model car (B) Bottom profile of the model car (C) Side profile of the model car.

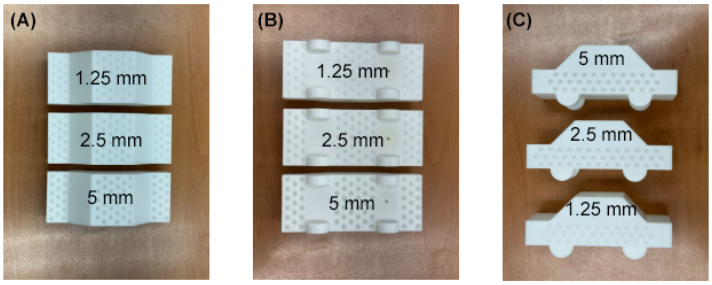

Figure 3: (A) Car models with top-surface dimpling (B) Car models with bottom-surface dimpling (C) Car models with side-surface dimpling.

increases with depth. The choice of V-shaped and semi-circular hybrid dimples instead of circular ones, like those on a golf ball, is due to the fact that golf balls typically experience normal airflow, where the airflow hits directly onto the ball and only small turbulent pockets are needed. In contrast, cars usually encounter tangential flow, where air slides along the body and surface. For this kind of streamlined, attached flow, a more controlled and directional vortex helps the air stay attached longer and reattach smoothly at the back. V-shaped dimples have proven to reduce drag at near tangential airflow, which is the primary type of airflow when cars are in motion (Chullai et al., 2019). Furthermore, circular dimples have also been shown to reduce drag under all conditions (Ali et al., 2024; Kaushik et al., 2018; Shaw et al., 2020). Additionally, the compound-shaped dimple design has been demonstrated to be more effective for cars, as it provides a smaller lift coefficient and L/D ratio (Paul et al., 2019). Therefore, by combining the features of V-shaped and circular dimples, overall performance could be enhanced.

Using dimple depths of 1.25 mm, 2.5 mm, and 5 mm provides a useful parameter sweep that spans from shallow (small perturbation) to moderate (stronger vortex generation) to deep (maximal disturbance). This allows for the detection of linear or non-linear trends in drag response, identifies an optimum, and checks for thresholds where negative effects, such as excessive skin friction drag, may arise. By placing these dimples in diagonal rows rather than in vertical or horizontal arrangements, airflow does not encounter perfectly aligned rows of disturbances. Instead, each dimple interacts differently, generating a series of staggered swirling vortices that move downstream along the car's surface rather than across it. Furthermore, when dimples are arranged in straight rows, the airflow tends to become trapped in the grooves between the rows, creating bands of alternating turbulent streaks. Diagonal arrangements also promote vortices that turn slightly sideways, creating cross-flow mixing that evens out velocity and pressure gradients.

To physically produce the models for wind tunnel testing, high-precision photocuring (SLA 3D printing) was used instead of conventional fused deposi-

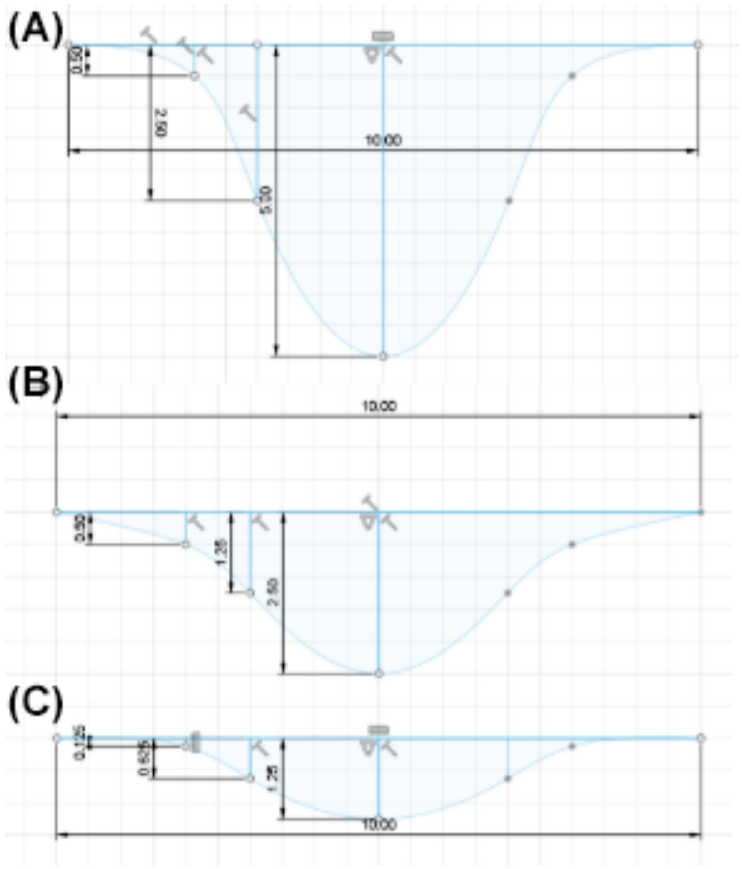

Figure 4: (A) Side profile of a dimple with a depth of 5 mm (B) Side profile of a dimple with a depth of 2.5 mm (C) Side profile of a dimple with a depth of 1.25 mm.

tion modeling (FDM) or other extrusion-based methods. Photocuring provides a smoother, more precise outcome, which can greatly affect aerodynamics if not achieved. Since geometric errors can greatly impact the results of the testing, the margin of error was set to ± 0.01 mm, ensuring that there are no layer lines that may produce uncontrolled turbulence.

3.2 Wind tunnel

The wind tunnel created is based on a subsonic wind tunnel design that includes a compressor/intake, a test section, and a diffuser/exhaust. An open-loop design was chosen instead of a closed-loop design to lower construction costs and complexity, as less material is required to maintain airflow. It also has a superior air inlet compared to closed-loop wind tunnels since its air supply is drawn from the external environment, ensuring a continuous flow of air. Additionally, it prevents the accumulation of exhaust products, which can interfere with measurements (Mangrulkar et al., 2019). The wind tunnel comprises three sections: the intake/compressor, the test section, and the exhaust/diffuser. The converging shapes of the exhaust and intake increase air velocity and reduce large-scale turbulence, creating a more uniform and laminar flow profile. The 17-degree angle provides a steep enough contraction to generate acceleration and pressure recovery while preventing boundary layers along the walls that may cause uneven flow. The test section features two mesh screens that straighten and smooth airflow before it reaches the model. Using two 0.5 cm mesh screens dissipates irregularities in airflow that may have been caused by uneven surfaces or external factors. The first layer of mesh disrupts and dissipates larger eddies, breaking them into smaller ones that can be further attenuated by the second mesh screen. After the mesh screens, a honeycomb structure composed of 6 cm straws forces air to move in the axial direction, which reduces turbulence intensity. The honeycomb structure has very high porosity, resulting in less pressure drop or energy loss while still preventing crossflow and swirls. This creates an even velocity field, ensuring that any changes in drag or lift are due to the model rather than irregularities in the airflow.

For the fan intake system, four 110V axial fans connected in parallel were used, each maintaining a spin rate of 2700 rpm and moving 112 CFM of air to increase the total volumetric flow rate. By placing the fan after the exhaust, the system pulls air into the test section instead of pushing it, utilizing negative pressure to draw air more uniformly. This arrangement ensures that the flow entering the section is evenly distributed across the model while preventing backflow and acoustic interference, leading to more accurate and controlled testing conditions.

3.3 Force balance

A force balance is essential in a wind tunnel experiment to accurately measure the aerodynamic forces acting on a model, such as lift and drag. It converts these physical forces into measurable electrical signals that can be recorded and

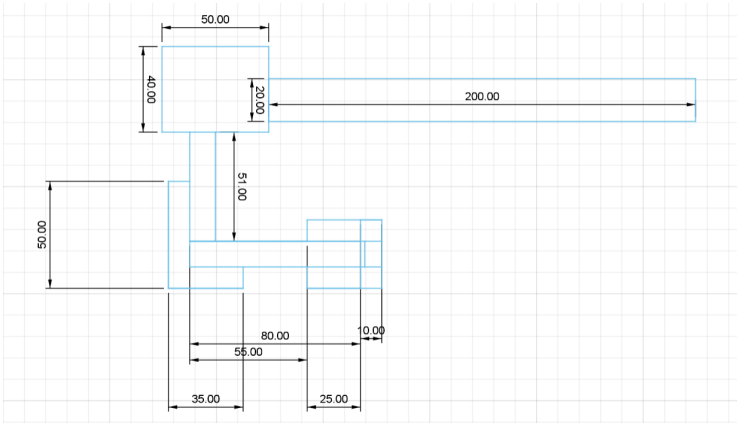

Figure 5: Force balance design diagram.

analyzed. Without a force balance, quantifying how air interacts with the object's surface would be impossible. By capturing these precise measurements, researchers can evaluate the model's aerodynamic performance, compare designs, and optimize shapes for efficiency and stability.

The force balance circuit consists of two SparkFun 220 load cells with a 10 kg load limit, two HX711 analog-to-digital converters and amplifiers (the HX711 serves both roles), and an Arduino Uno board to quantify drag and lift during the experiment. The load cells are $1.2 \times 1.2 \times 7.5$ cm aluminum cuboids with strain gauges built into them, so that when pressure is exerted on one side, the load cell generates a small signal swing proportional to the force applied. However, load cells only measure force in one dimension; therefore, to measure both lift and drag, two load cells are required. Furthermore, load cells are typically paired with HX711 amplifiers because the signal swings are too small for computers to detect. The HX711 amplifies the signal swing and converts the analog signal to digital. The Arduino Uno board acts as a central processing unit, sending the signal results to the computer. The programming for the circuit is done using the Arduino IDE (Figure. 5).

The actual force balance structure is assembled using 3D-printed frames, with each load cell secured along the x-axis and y-axis to measure lift and drag, respectively. A string is attached to the end of the load cell frames and extends into the wind tunnel, where it connects to the car. As the car moves, a corresponding force vector, which can be separated into lift and drag, is applied to the load cell, generating an appropriate signal swing that can be detected by the computer (Weakly et al., 2024).

Before assembling the actual force balance, it is necessary to calibrate the load cells. Calibration is essential because, although the strength of the signal swing is proportional to the force applied, the relationship between the signal swing and the force is unknown and varies for each load cell. Calibration involves placing a known mass or exerting a known amount of force on the

load cell, recording the reading, and using the formula $Calibration\ Factor = \frac{reading\ of\ the\ load\ cell}{Known\ mass/known\ force}$ to determine the calibration factor. Finally, the calibration factor is inserted into the code so that every time an electrical signal is generated, it is multiplied by this factor. By calibrating the load cell, the readings obtained will be in grams or newtons, depending on the unit used for the conversion of the original reading of the cell.

3.4 Computational fluid dynamics (CFD) analysis

For CFD analysis, Autodesk CFD is used to simulate fluid dynamics and obtain data for comparison with real wind tunnel results. The parameters of the wind tunnel in the CFD simulation are approximately the same as those of the observation box, which measures around 20×20×50 cm. The wind speed is also equivalent to that of the real wind tunnel, at 2.7 m/s. Furthermore, the conditions used are standard temperature and pressure (1 atm and 26 degrees Celsius). Additionally, CFD provides detailed insights into how airflow interacts with the car body and reveals the wind speed distribution on a plane when the wind strikes the car. By using CFD, a better understanding of the fluid dynamics differences between dimpled vehicles and conventional car bodies is achieved.

3.5 Reynolds number

The Reynolds number (Re) is calculated using the equation $Re = \frac{\rho u L}{\mu}$, where ρ = fluid density (kg/m^3), u = flow velocity (m/s), L = characteristic length of the object (m), and μ = dynamic viscosity of the fluid (Pa·s). Re indicates whether the flow will be laminar or turbulent. Every flow (e.g., water flow, air flow) has a critical Re that serves as the boundary between turbulent and laminar flow. When Re exceeds the critical value (commonly 2300, used as a standard when not measured during pipe testing), the flow becomes turbulent and is characterized by disturbed airflow. The higher the Re, the more turbulent the flow becomes. Conversely, when Re is below the critical value, the flow is laminar, exhibiting smooth and undisturbed characteristics; the closer Re is to zero, the more the flow approaches perfect laminar flow. A simple example of laminar and turbulent flow is running tap water: when the flow is laminar, the stream is transparent and smooth, indicating that Re is below the critical value. In contrast, when the flow is turbulent, it becomes translucent and rough, indicating that Re is above the critical value (Saldana et al., 2024). Although dimples do not directly impact Re, they can have varying effects under different types of flow that correlate with Re. Re is important to the experiment because it depends on the size of the vehicles; thus, using smaller models results in a smaller Re compared to real cars. Consequently, the flow behavior in the models may differ from that of real cars. To ensure that the dimples would be effective on real cars, Re must be maintained at a value close to that of real cars (Gattere et al., 2022).

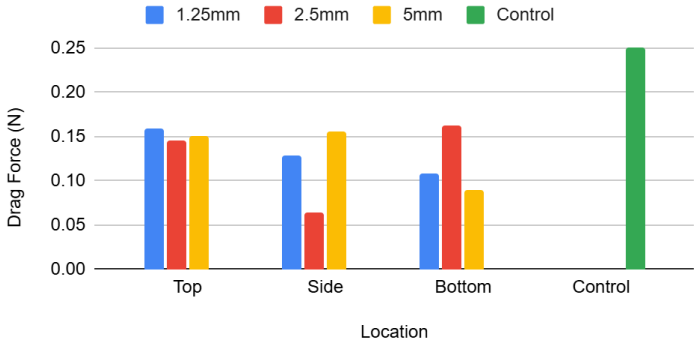

Figure 6: Wind tunnel: effect of dimple location and depth on drag force.

4 Results

The results of the drag forces within the wind tunnel at a wind speed of 2.7 m/s show how each combination of location and depth affects drag (Figure. 6). It is evident that the control model has significantly higher drag forces compared to those with biomimetic dimpling, confirming that smooth surfaces promote larger flow separation zones behind the model, resulting in higher drag. Models with dimpling at the top exhibit a consistent drag force across all dimple depths but still noticeably lower drag forces than the control model. This indicates that once the boundary layer at the top transitions to turbulence, further deepening of the dimples offers diminishing returns. The top dimples primarily interact with the freestream air that travels fastest due to stagnation at the car's leading edge. The increased attachment of airflow to the car's surface raises skin friction, offsetting the overall drag reduction effect. In models where dimples were located on the sides, the effect was most significant at the 2.5 mm depth, where drag dropped to a third of the drag force of the control model. This also indicates an optimal dimple depth: if the dimples are too shallow, there isn't enough vortex recirculation, and if they are too deep, they overly disturb the boundary layer, causing early re-separation. Conversely, when the dimples were located at the bottom of the vehicle, the effects were less consistent. This may be explained by the low-pressure flow beneath the model, where airflow is constrained by the model and the tunnel floor, forming a highly turbulent region. Furthermore, gravitational effects reduce the time the air spends in contact with the dimples, limiting the benefits of vortex generation and increasing skin friction drag.

The data also show that dimples affect vertical pressure distribution (Figure. 7). Using the control model as the baseline for the amount of lift generated, there is an increase in lift when the dimples are placed on the top. This is due to the airflow moving faster at locations with dimpled surfaces, creating a lower pressure zone at the top of the car, which increases the pressure difference and

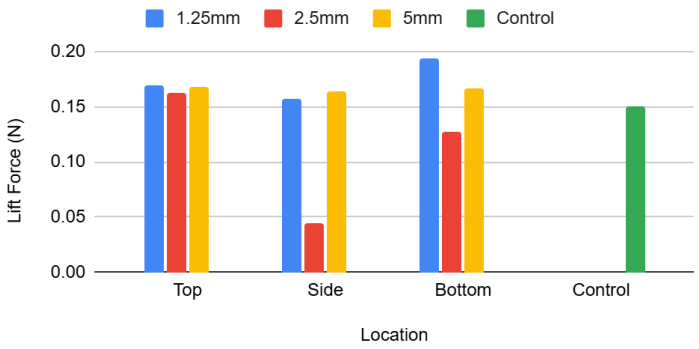

Figure 7: Wind tunnel: variation of lift force with dimple location and depth.

generates lift. In contrast, when the dimples are located at the bottom, the lift force is inconsistent due to the more turbulent airflow near the bottom. When the dimples are placed at the bottom with a depth of 2.5 mm, they generate downforce, likely due to a decrease in the pressure gradient as air moves faster along the bottom, creating a lower pressure that matches the top. When the dimples are placed on the sides, they have a more balanced effect, redistributing lateral airflow without significantly affecting lift. However, there is an anomaly with side dimples at a depth of 2.5 mm, where there is a significant increase in downforce.

The mean velocity results from the CFD further show how the placement and depth of dimples affect airflow behavior along the surfaces (Figure. 8). When the dimples are placed on the sides, there is a clear optimum at 2.5 mm. This pattern indicates that moderate-depth dimples on the sides create the most effective streamwise vortices, pulling higher-energy air from the freestream into the near-wall region and thereby thinning the boundary layer. When the dimple depth is either deeper or shallower than the optimum, there is a decrease in the mean velocity of the airflow. This may be due to insufficient vortex generation in the shallow dimples and excess skin friction drag, which can lead to dissipative effects. In contrast, if the dimples are placed at the bottom, the effects are lowest at 2.5 mm but overall have the least impact. This may be attributed to the close proximity of the surface to the ground and lower dynamic pressure, which limits vortex generation and makes the results more inconsistent. Aside from the anomalous 50 cm/s mean with the top 1.25 mm dimples, it shows similar but slightly lower results than the side dimples.

The pressure contours from the CFD simulation illustrate how dimpling affects airflow and influences skin friction and pressure drag (Figure. 9). The top dimples display a consistent decline in pressure as depth increases: around 2900 Dyne at 1.25 mm to just under 2500 Dyne at 5 mm. This steady reduction implies that deeper top-surface dimples cause greater flow disruption, leading to localized low-pressure zones and potentially earlier separation. Since the top

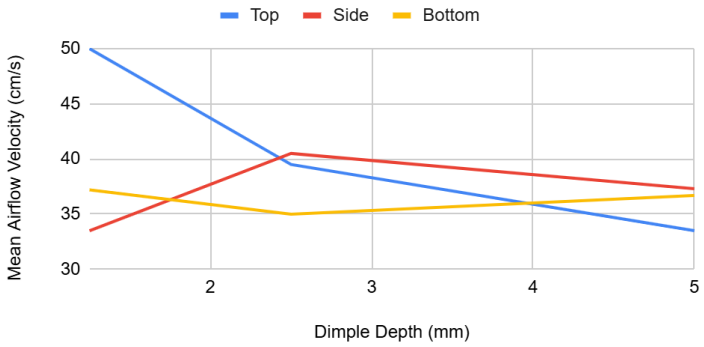

Figure 8: CFD analysis: variation of mean airflow velocity with dimple depth.

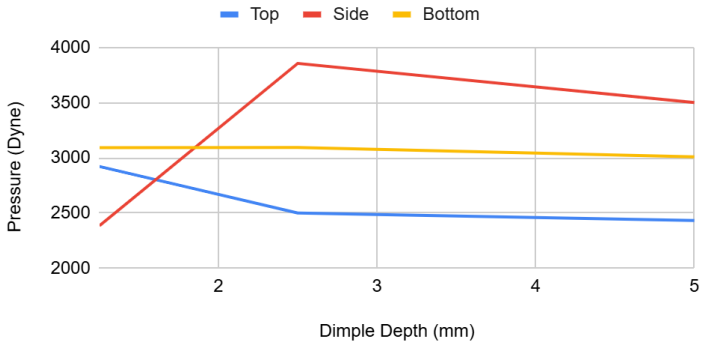

Figure 9: CFD analysis: variation of surface pressure with dimple depth.

region experiences faster airflow and higher dynamic pressure, excessive surface disturbance increases turbulence intensity without improving wake pressure recovery. The bottom surface tends to remain stable at all depths, suggesting that the depth of dimples on the bottom of the vehicle contributes minimally to pressure recovery. When the dimples are placed on the sides, there is an optimum for pressure recovery at 2.5 mm, where it is significantly higher than at other locations and depths. This is likely due to an optimal balance between boundary layer re-energization and minimal flow disruption. At this depth, the vortices are more controlled and delay separation, contributing to a smaller wake and lower overall drag effects.

In this comparison between the control model and the model with side dimples of 2.5 mm depth, it is evident that there is a smaller wake at the rear of the car, indicating a reduced pressure gradient due to improved pressure recovery (Figure. 10). This demonstrates the effect of biomimetic dimpling on wake size and airflow reattachment, significantly improving the vehicle's aerodynamics and reducing drag.

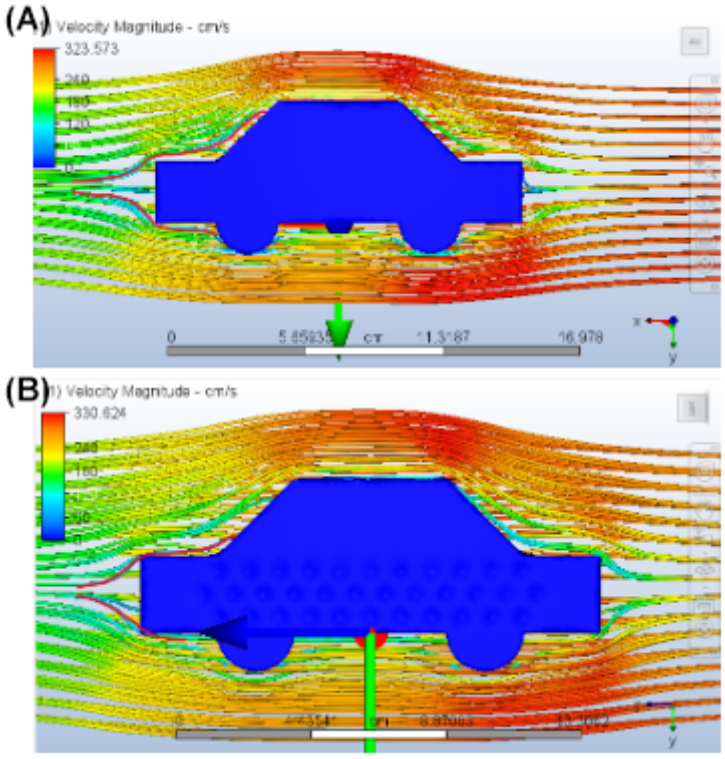

Figure 10: Images from CFD streamline showing the difference in wake size: (A) Control model (B) Side-surface dimpling 2.5 mm.

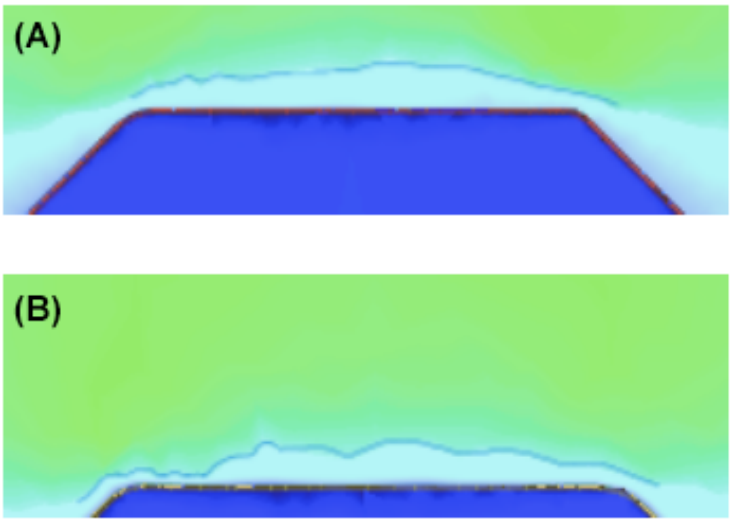

Figure 11: Diagram of airflow velocity on the roof of a car: (A) Control model (B) Top-surface dimpling 2.5 mm.

In this comparison of velocity magnitude contours between the control model and the model with top dimples of 2.5 mm depth, it is clear that the dimples create a turbulent boundary layer, resulting in irregularities in airflow along the surface (Figure. 11). In the control model, the airflow is smooth and laminar, leading to early detachment and separation from the surface, while the dimpled surface has a later separation point, reducing the wake and ultimately decreasing drag.

Overall, the comparison between the wind tunnel tests and the simulations shows strong qualitative agreement, confirming the reliability of the numerical model and the aerodynamic principles behind the dimple design. Both sets of results indicate that the model with a side dimple depth of 2.5 mm represents the optimal configuration. This setup produces the lowest drag while maintaining the greatest stability in lift, with controlled vortices that energize the boundary layer and promote smoother reattachment of airflow behind the car.

5 Discussion

5.1 Anomalies in the experiment

Certain anomalies have been found in the findings, including a sudden increase in downforce for side 2.5 mm dimples. This increase in downforce may be a result of pressure redistribution or measurement error. V-shaped and semi-circular hybrid dimples along the side may create small streamwise vortices that spiral along the car's surface, pulling high-energy air from the top

to the sides, reducing pressure at the upper surface and generating local suction that increases downforce. Another possibility is an experimental error. At low Reynolds number regimes, small changes in geometry or experimental setup lead to disproportionately large effects on turbulence transition. To verify which theory is accurate, referring back to CFD simulation results allows for a better understanding of the anomaly. In the CFD, side 2.5 mm dimples have an approximate downforce of 0.74 N, while side 1.25 mm dimples only have a downforce of 0.13 N. This validates the aerodynamic explanation for this anomaly, where the V-shaped and semi-circular hybrid dimples hit an aerodynamic sweet spot, energizing the boundary enough to prevent detachment and maintain a smoother downward flow that increases stability and pressure differentials.

Another anomaly found in the findings was a sudden spike in the mean velocity of the top 1.25 mm dimples within the CFD simulation. It is possible that strong local jetting or flow channeling may create an increase in mean velocity, but such a large spike usually indicates a measurement error. A plausible explanation for this anomaly is that the simulation captures an instantaneous snapshot of the mean velocity within the wind tunnel, possibly reflecting a transient peak and causing the sudden spike.

5.2 Practical and engineering applications

The findings have important applications for future automotive aerodynamic design. Reducing drag on vehicles not only decreases fuel consumption in gas-powered cars but also increases efficiency in future electric vehicles. The extent to which these drag reductions benefit the vehicles can be translated into real-world impacts. For example, if side dimples with a depth of 2.5 mm, which reduce drag by up to 25%, were to be produced and computed with the corresponding C_d, along with geometric scaling caveats, the estimated energy savings for a standard car can be calculated using the formula $P = F_D V = \frac{1}{2}\rho C_d A V^3$. A slight reduction in C_d results in cubic speed-amplified savings, which is compelling for long-distance travel and EV range extension.

The findings also demonstrate that full-body dimpling is not required to achieve maximal benefits in drag reduction. Implementing dimples in specific locations where flow separation is most pronounced may yield a far greater cost-to-benefit ratio. Integrating V-shaped and semi-circular hybrid dimple textures into vehicle surfaces is increasingly feasible with modern automotive manufacturing technology. The dimples can be implemented using various methods, including automotive metal stamping. This technique is a high-speed manufacturing process that uses hydraulic or mechanical presses to mold metals into precise, complex vehicle components like body panels. This method is efficient and can be performed in mass production, allowing for large outputs for commercial car use. However, producers must also address durability challenges. Dimples, especially those with sharper geometries like V-shaped and semi-circular hybrids, may accumulate dust, ice, and water over time, degrading both aerodynamic and aesthetic performance. To combat this challenge, surfaces should incorporate hydrophobic coatings and self-cleaning technologies, such as nanos-

tructured materials, to repel debris. Additionally, they must withstand harsher erosion since dimples generate higher skin friction drag, which may cause parts to wear out faster.

5.3 Limitations of the experiment

While this experiment shows promising data for future automotive engineering, there are certain limitations that may influence real-world applications. Firstly, the car model is a scaled-down version, leading to lower Reynolds numbers that alter flow transition points compared to full-sized cars, where airflow behaves more viscously, with a thicker boundary layer and an earlier transition from laminar to turbulent flow. In this experiment, the Reynolds number is 2.7×10^5 for the wind tunnel and 3.5×10^5 for CFD, while in real life, the Reynolds number for cars is around 1×10^6 to 3×10^6 (Keiyinci et al., 2024). As a result, flow separation, vortex formation, and wake characteristics may behave differently under full-scale conditions. At low Reynolds numbers, dimples induce turbulence prematurely. At higher Reynolds numbers, they more effectively re-energize the boundary layer, reducing the wake region. This means that the drag reduction observed in the scaled-down model is qualitatively valid, but exact quantitative improvements cannot be fully determined without high Reynolds number simulations. Secondly, the model used was designed as a generalized commercial vehicle rather than a detailed reproduction of a specific model. The shell features mostly flat and planar surfaces rather than the complex curvatures and designs of modern vehicles. Real cars have curves that help ensure a smoother transition and reduce flow separation. The flat-sided model creates sharp edges that may exaggerate separation points that might not exist in full-scale models. The simplification was intentional to allow for consistent dimple placement and eliminate other confounding factors, but it inevitably alters the flow physics. Therefore, while the model provides insights into how localized turbulence affects the aerodynamic performance of a car, the actual drag coefficients are not representative of a real automobile body. Lastly, although the wind tunnel testing and CFD testing were used for cross-validation, they produce inherent uncertainties. In the sting, turbulence modeling assumes isotropic turbulence, which may not accurately reproduce the small-scale anisotropic turbulence present in the wind tunnels.

6 Conclusions & Future Work

6.1 Research conclusions: advancing sustainable mobility through biomimetic engineering

This study successfully validates the critical role of biomimetic dimple technology in vehicle aerodynamic optimization, providing an innovative solution for sustainable transportation. Through systematic parametric analysis, we have identified that side-mounted dimples with a 2.5-mm depth deliver optimal drag

reduction performance, achieving a 25% reduction in resistance. This finding carries significant implications for sustainable development:

First, as a passive energy-saving solution, this technology enhances energy efficiency without the need for external power input, perfectly complying with the objectives of SDG 7, "Affordable and Clean Energy." For electric vehicles, this translates to an extended driving range with the same battery capacity, effectively alleviating range anxiety. For conventional vehicles, it directly reduces fuel consumption and carbon emissions.

Second, our "localized optimization" design philosophy embodies the principle of resource minimization. By applying dimples only to critical areas, we achieve significant benefits while avoiding the resource consumption associated with full-vehicle modifications, making it highly compatible with circular economy principles.

Most importantly, this technology provides an immediately feasible transition solution applicable to both new vehicle manufacturing and existing vehicle retrofitting, enabling conventional fleets to improve energy efficiency right away and contributing substantially to the low-carbon transition of the transportation sector.

6.2 Future perspectives: building a technical roadmap for sustainable transportation

To translate research findings into tangible sustainability benefits, we propose the following development pathway:

- Establishing a Life Cycle Assessment Framework

Next-phase research will employ carbon footprint tracking and energy investment return analysis to precisely quantify the environmental benefits of dimple technology across manufacturing, usage, and recycling stages, ensuring a positive net sustainability outcome.

- Developing Green Manufacturing Processes

We will explore the use of recycled materials and low-carbon processes to produce dimple structures while investigating integration solutions with lightweight vehicle bodies to minimize environmental impact at the source.

- Promoting Cross-Sectoral Integration Applications

Future work will investigate the technology's potential applications in public transportation systems, including electric buses and freight trucks, to expand its decarbonization impact. Concurrently, we will explore synergistic effects with other clean technologies, such as solar roofs.

- Developing Policy Promotion Models

We will establish carbon reduction benefit prediction models to provide a scientific basis for governments formulating vehicle efficiency standards and subsidy policies, accelerating technology adoption.

Overall, this research demonstrates the value of nature-inspired engineering innovation in addressing sustainable development challenges. By combining biomimetic principles with sustainable engineering, we have not only pioneered a new approach to vehicle energy conservation but also provided a concrete and feasible technical solution for building green transportation systems.

7 Acknowledgement

The authors sincerely appreciate Miss Irene Liang for her outstanding assistance with the experiments.

8 References

Alam, F., Steiner, T., Chowdhury, H., Moria, H., Khan, I., Aldawi, F. et al. (2011) *A study of golf ball aerodynamic drag.* Procedia Engineering, 13, 226–31. https://doi.org/10.1016/j.proeng.2011.05.077

Ali, H., Rasani, M.R., Harun, Z. and Shahid, M.A. (2024) *Passive flow-field control using dimples for improved aerodynamic flow over a wing.* Scientific Reports, 14, 12918. https://doi.org/10.1038/s41598-024-63638-z

Ali, H., Rasani, M.R. and Harun, Z. (2025) *Impact of the dimple indentation depth and location for passive flow control in Blended Wing Body airframe at low and high subsonic speeds.* PLOS One, 20, e0325778. https://doi.org/10.1371/journal.pone.0325778

Ballerstein, N. and Horst, P. (2023) *Manipulation of the aerodynamic behavior of the DrivAer model using dimple patterns.* Journal of Wind Engineering and Industrial Aerodynamics, 233, 105216. https://doi.org/10.1016/j.jweia.2022.105216

Chullai, E.T., Singh, J., Chandel, A. and Singhal, U. (2019) *Effects of V-shaped dimples on NACA 0012 airfoil.* Hindustan University. https://www.academia.edu/26479093/Effects_of_V

Gattere, F., Chiarini, A. and Quadrio, M. (2022) *Dimples for skin-friction drag reduction: status and perspectives.* Fluids, 7, 240. https://doi.org/10.3390/fluids7070240

Kacem, A. and Abdullah, A.N. (2016) *Determination of drag coefficient for Pajero car model (Using Strain Gauge Method).* IOSR Journal of Mechanical and Civil Engineering, 6, 18–23. https://www.iosrjournals.org/iosr-jmce/papers/vol13-issue6/Version-3/D1306031823.pdf

Kaushik, V., Mahore, M. and Patil, S. (2018) *Analysis of dimpled wing of an aircraft.* International Journal of Engineering Development and Research, 6, 382–395. https://rjwave.org/ijedr/papers/IJEDR1803068.pdf

Keiyinci, S., Bas, O. and Akar, M.A. (2024) *Investigation on flow characteristics of generic car body with different boundary conditions.* Scientia Iranica, 31, 1077–1089. https://doi.org/10.24200/sci.2023.59961.6523

Li, X., Tan, Y., Qiu, X., Gong, Z. and Wang, M. (2021) *Wind tunnel measurement of aerodynamic characteristics of trains passing each other on a simply supported box girder bridge.* Railway Engineering Science, 29, 152–62. https://doi.org/10.1007/s40534-021-00231-4

Mangrulkar, A.L., Bagade, S., Chavan, S., Babani, J. and Bhagat, S. (2019) *Design and fabrication of an open circuit subsonic wind tunnel for educational purposes.* International Research Journal of Engineering and Technology, 6, 1271–1275. https://www.irjet.net/archives/V6/i4/IRJET-V6I4270.pdf

Mat, A.A.M., Taib, I., Mahbubi, M., Jefri, W.N.A.A.W., Teor, W.H. and Mansoor, B. (2025) *Analysis of aerodynamics on surface of the car with turbulence models.* Semarak Journal of Thermal Fluid Engineering, 4, 35–51. https://doi.org/10.37934/sjotfe.4.1.3551a

Obayashi, S., Jeong, S., Chiba, K. and Morino, H. (2007). *Multi-objective design exploration and its application to regional-jet wing design.* Transactions of the Japan Society for Aeronautical and Space Sciences, 50, 1–8. https://www.jstage.jst.go.jp/article/tjsass/50/167/50_167_1/_pdf

Palanivendhan, M., Chandradass, J., Saravanan, C., Philip, J. and Sharan, R. (2021) *Reduction in aerodynamic drag acting on a commercial vehicle by using a dimpled surface.* Materials Today: Proceedings, 45, 7072–7078. https://doi.org/10.1016/j.matpr.2021.01.884

Paul, S., Paul, A. and Koly, F.A. (2019) *A review of different shaped dimple effects on aerofoil surfaces.* Proceedings of the International Conference on Mechanical Engineering and Renewable Energy 2019, PI-168. https://www.researchgate.net/publication/337893765_A_REVIEW_OF_DIFFERENT_SHAPED_DIMPI

Saldana, M., Gallegos, S., Gálvez, E., Castillo, J., Salinas-Rodríguez, E., Cerecedo-Sáenz, E. et al. (2024) *The Reynolds number: a journey from its origin to modern applications.* Fluids, 9, 299. https://doi.org/10.3390/fluids9120299

Shaw, K.K., Kesarwani, Y. and Chakravarty, P. (2020) *Study of dimple effect on aerodynamic drag characteristics of a car.* International Journal of Innovative Research in Science Engineering and Technology, 9, 4628–4637. https://www.researchgate.net/publication/343826450_Study_of_Dimple_Effect_on_Aerodynamic_Drag_C

Tarakka, R., Salam, N., Mochtar, A. A., Rauf, W. and Ihsan, M. (2023) *On the aerodynamics of rear of vehicle model with active control by blowing: computational and experimental analysis.* International Journal of Mechanical Engineering and Robotics Research, 12, 84–90. https://www.ijmerr.com/2023/IJMERR-V12N2-84.pdf

Weakly, J., Ho, S., Feehery, E., Kothmann, B. and Sung, C. (2024) *A low-cost, adaptable system for lift and drag measurement in an educational wind tunnel.* 2024 ASEE Annual Conference & Exposition Proceedings. https://doi.org/10.18260/1-2–46453

Yu, H., Huang, Y., Wang, Y., Qian, Y. and Fu, S. (2023) *Flow field analysis of a turbulent channel controlled by scalloped riblets.* Aerospace Research Communications, 1, 12300. https://doi.org/10.3389/arc.2023.12300